Steel and Composite Structures, Vol. 10, No. 5 (2010) 385-414
DOI: http://dx.doi.org/10.12989/scs.2010.10.5.385

Finite element evaluation of the strength behaviour of high-strength steel column web in transverse compression

Ana M. Girão Coelho*[1,2] and Frans S.K. Bijlaard[1]

[1]*Department of Structural and Building Engineering – Steel and Timber Structures*
Faculty of Civil Engineering and Geosciences, Delft University of Technology
PO Box 5048, 2600 GS Delft, The Netherlands
[2]*Institute of Computers and Systems Engineering of Coimbra (INESC-Coimbra),*
Rua Antero de Quental 199, 3000-033 Coimbra, Portugal

(Received October 13, 2009, Accepted June 7, 2010)

Abstract. In current European Standard EN 1993, the moment-rotation characteristics of beam-to-column joints made from steel with a yield stress > 460 MPa are obtained from elastic design procedures. The strength of the joint basic components, such as the column web subject to local transverse compression, is thus limited to the yield resistance rather than the plastic resistance. With the recent developments of higher strength steel grades, the need for these restrictions should be revisited. However, as the strength of the steel is increased, the buckling characteristics become more significant and thus instability phenomena may govern the design. This paper summarizes a comprehensive set of finite element parametric studies pertaining to the strength behaviour of high-strength steel unstiffened I-columns in transverse compression. The paper outlines the implementation and validation of a three-dimensional finite element model and presents the relevant numerical test results. The finite element predictions are evaluated against the strength values anticipated by the EN 1993 for conventional steel columns and recommendations are made for revising the specifications.

Keywords: column web in compression; component method; connections; eurocode 3(en 1993); finite element method; high-strength steel; joints; strength.

1. Introduction

The steel industry has recently made an effort to re-engineer structural steels to have improved performance in tensile stress, toughness, weldability and corrosion for use in bridge and building applications. This has led to the development of a new class of steels, generally classified as high-strength steels (minimum yield strength greater than 460 N/mm^2). The material properties of high-strength steels are different from mild carbon steel in several key areas of the uniaxial stress-strain relationship as can be seen in Fig. 1. This figure shows that these steels have neither a well-defined yield plateau nor a substantial strain-hardening modulus as compared with mild steel S355. In general, high-strength steels are also less ductile than mild steels. These characteristic differences in the mechanical properties of high-strength steels are at issue in light of the assumptions that the current

* Corresponding author, Ph. D., E-mail: a.m.girao@clix.pt

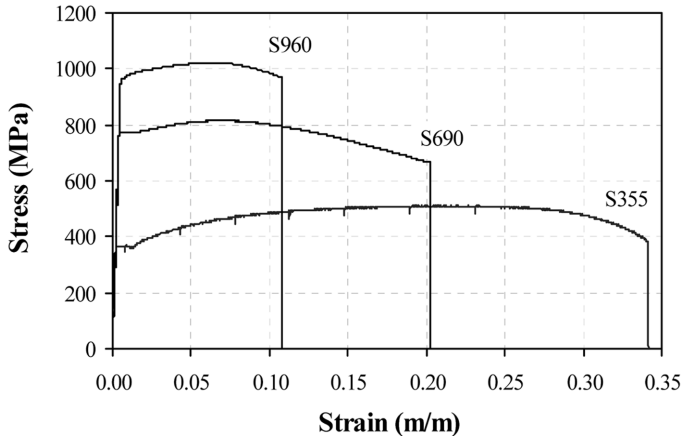

Fig. 1 Stress-strain characteristics of structural steels tested by the authors

European code of practice for the design of steel structures (EN 1993) makes in its prediction of the ultimate response of structural members and joints (CEN 2005a,b). Part 1-12 of EN 1993 (CEN 2005c), which specifically deals with the design rules for members and joints made from these new classes of steel, does not permit inelastic design procedures for such elements because there is no background research work that shows that these accommodate plastic deformations. The tests described in this paper form part of a research programme into the behaviour of members and joints fabricated from high-strength steel, from strength and ductility standpoints. The aim of the programme is to investigate whether members and joints with yield stresses in the range from 460 MPa to 960 MPa can be designed according to existing rules of the EN 1993 or whether these rules need to be modified to include high-strength steel. These objectives are addressed below through detailed nonlinear finite element (FE) analyses of joint components.

High-strength steels are most efficient when they develop their full yield stress, *i.e.*, when structural elements are designed on the basis of strength. Research studies at Delft University of Technology (Girão Coelho *et al*. 2007a, b, 2009, 2010) have indicated that the benefits of the use of these steels can be utilized in plastically designed braced frames, for which stiffness, in the form of deflections or drift limits for complying with serviceability limit states, does not govern design. EN 1993 adopts the semi-continuous/partially-restrained philosophy for the design of this type of framing in recognition of the economic benefits. Semi-continuous frame design however requires the modelling of beam-to-column joints.

The characteristics of a beam-to-column joint are best described by the moment-rotation relationship. Current design practice adopts the component method for predicting this relationship. The design basis consists of first identifying all active components for a given structural joint, including the fasteners, column web panel in shear, column web in transverse compression caused by bearing, etc. The individual component force-deformation response is then characterized and finally those elements are assembled in the form of a mechanical model made up of extensional springs and rigid links. This spring assembly is treated as a structure whose force-deformation behaviour is used to generate the moment-rotation curve of the full joint. Recently, Skejic *et al*. (2008) conducted a reliability analysis of welded beam-to-column joints designed to EN 1993-1-8. The authors demonstrated the high reliability level of the component-based design procedure adopted in the code. Simões da Silva (2008) further extended the concept to

develop a three-dimensional conceptual model for the design of joints.

In many steel and composite designs it is common for the compression zone in the column web to be loaded to such an extent that it governs the design of the joint. Failure of the column web in compression can develop due to crushing of the web close to the flange (bearing mechanism) and/or buckling (plate buckling phenomenon). Most practical column webs fail by crushing. As the load increases further, to the crushing resistance and beyond, the column web carries additional loading and eventually buckles. Inelastic buckling is essentially a secondary effect. However, as the strength of the steel is improved, buckling characteristics become more dominant and the web capacity may be controlled by local buckling.

The main factors on which the strength characteristics of a column web in transverse compression depend are (i) web thickness, (ii) web slenderness, (iii) material properties and (iv) level of axial load and shear in the column. In this research, high-strength steel I-columns with different geometrical and mechanical properties are considered. The web slenderness is varied in such a way that the progression to failure is representative of the possible collapse mechanisms of a web in transverse compression. The effect of axial load and shear is not considered below.

The current paper starts with a review of the EN 1993 design specifications for unstiffened column web in compression. The next section describes the analysis configurations utilized in this research and identifies the key design variables that influence the behaviour of the joint component. The FE model used in the study is then formulated and results are presented and discussed. Comparisons between FE predictions and the values anticipated by the EN 1993 for conventional mild steels are drawn. It is shown that current design provisions are applicable to columns fabricated from high-strength steel.

2. EN 1993-1-8 design rules for mild steels

Previous research pertaining to the behaviour of the component column web in compression includes investigations by Aribert *et al*. (1977, 1981, 1990), Zoetemeijer (1980), Witteveen *et al*. (1982), Jaspart (1991, 1997), Weynand *et al*. (1995), Kuhlmann and Kühnemund (2000a, 2002), Kühnemund (2003) and De Mita *el al*. (2008). Several relationships between the force and deformation of a web in transverse compression have been proposed for monotonic loading and have been adopted in design codes. EN 1993-1-8 gives rules for evaluation of resistance and elastic stiffness based on plastic and elastic theories, respectively. The related provisions are summarized below and their background is detailed in Appendix 1.

2.1 Resistance formulae

The design resistance of the column web in compression $F_{c,wc,Rd}$ is taken as the smaller of the two following resistances: (i) crushing resistance and (ii) buckling resistance. The crushing resistance is given by

$$F_{c,\,wc,\,Rd} = \frac{\omega k_{wc} b_{eff,\,c,\,wc} t_{wc} f_{y,\,wc}}{\gamma_{M0}} \tag{1}$$

where ω : reduction factor for interaction with shear; k_{wc}: reduction factor for interaction with compressive stress in the column; $b_{eff,c,wc}$: effective width that accounts for the spreading of the compressive force transferred by the beam compression flange in bearing; t_{wc}: column web thickness; $f_{y,wc}$: yield stress of the column web; and γ_{M0}: partial safety factor (c.f. Appendix 1).

The column web must also be checked for buckling. Web failure of this type is treated as a plate buckling problem. In this respect, EN 1993-1-8 proposes the following formula, which is based on the stability studies of the column web in compression undertaken by Aribert *et al*. (1990) and Jaspart (1991)

$$F^{*}_{\mathrm{c,wc,Rd}} = \frac{\omega k_{\mathrm{wc}} \rho b_{\mathrm{eff,c,wc}} t_{\mathrm{wc}} f_{\mathrm{y,wc}}}{\gamma_{\mathrm{M1}}} \leq F_{\mathrm{c,wc,Rd}} \tag{2}$$

where ρ: reduction factor for plate buckling ($0 \leq \rho \leq 1$); and γ_{M1}: partial safety factor (c.f. Appendix 1).

2.2 Stiffness formulae

According to EN 1993-1-8, the elastic stiffness coefficient of the column web in compression k_2 is obtained as

$$k_2 = \frac{0.7 b_{\mathrm{eff,c,wc}} t_{\mathrm{wc}}}{d_{\mathrm{wc}}} \tag{3}$$

being d_{wc}: clear depth of the column web. The background to this formula is given in Appendix 1.

2.3 Ductility characteristics

EN 1993-1-8 does not give any quantitative guidance on the characterization of the deformation capacity and ductility of the column web in compression. This component is generally classified under limited ductility because local instability phenomena often govern the ultimate behaviour (Jaspart 1997, Kuhlmann *et al*. 1998).

3. Test configuration and parameters

The geometries of the analysis configurations utilized in this research are derived from the geometry of previous I-beam specimens fabricated from high-strength steel plates and tested by the authors (Girão Coelho *et al*. 2009) (Fig. 2a). Different analysis configurations are created by changing some of the attributes of both specimens. Important geometric and mechanical parameters are varied over the practical range of interest in order to evaluate the behaviour of the web under transverse compression.

A generic configuration for the FE numerical tests performed in this research is shown in Fig. 2b. Specific characteristics and attributes modelled in these studies are as follows

- all tests involve uniaxial transverse compression to simulate the behaviour of two sided symmetric joints ($\beta = 0$);
- the load is applied directly to the column flange – Zoetemeijer (1980) has shown that the influence of the load strip length is negligible;
- the geometric imperfections are modelled based on EN 1090-2 tolerances (CEN 2008);
- residual stresses due to welding are not accounted for;
- the effect of column axial load is not taken into consideration.

Variables considered in the parametric studies are

- cross-section based variables: web thickness t_{wc}, flange thickness t_{fc} and out-of-flatness of the web;

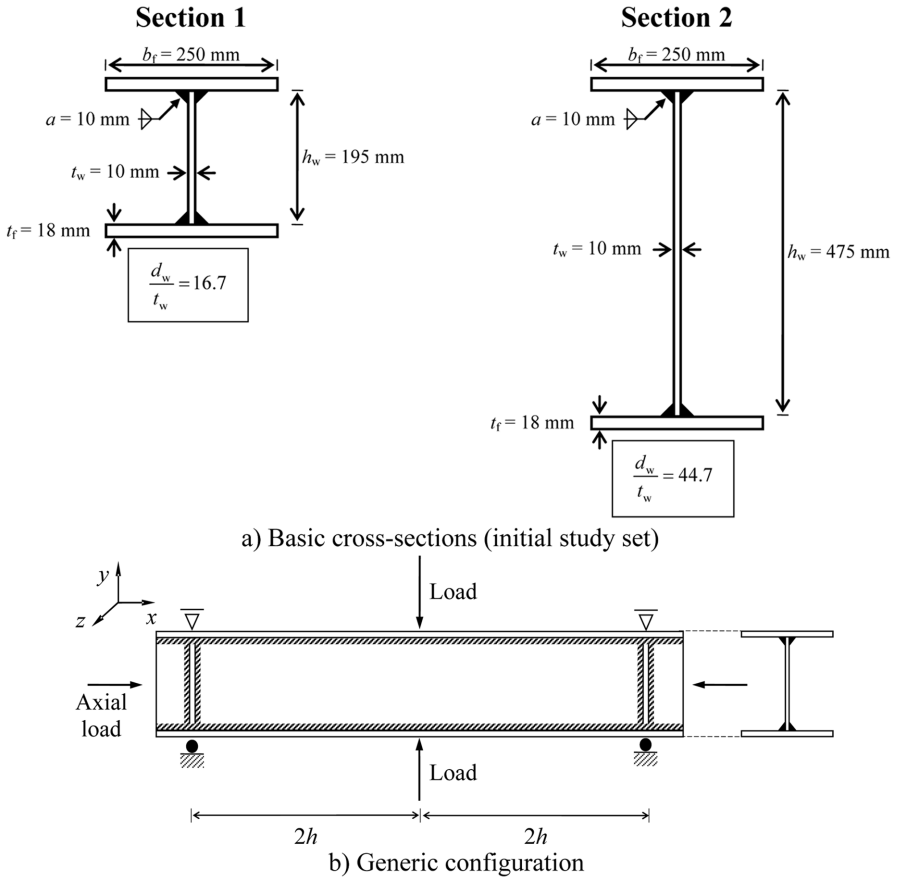

Fig. 2 Test configuration for the FE tests

· steel mechanical properties: steel grades S690 and S960.

The specific values of the above variables considered within the parametric studies are given in Table 1 (b: section width; h: section height; $f_{y,nom}$: nominal yield stress). The configurations are divided into three series, each focusing on a different geometric parameter. All tests are conducted using steel grade S690 and S960. The main variable in series WT is the column web thickness, which affects the web plate slenderness. Hence, series WT focuses on the effect of column web thickness on inelastic behaviour of the compression zone of a column web. Similarly, series FT focuses on the effect of flange thickness, while series WI is centred on the effect of the web imperfection (out-of-flatness).

4. Finite element model

Virtual numerical tests were performed with the commercial FE package LUSAS (FEA 2006) with the following objectives: (i) to investigate the general strength behaviour of the compression zone of column webs, (ii) to characterize the relevant failure modes and (iii) to discuss and compare preliminary results with the predictions anticipated by EN 1993-1-8.

Table 1 Summary of FE parametric studies (Continued)

Test	Geometric properties					Out-of--flatness	$f_{y,nom}$ (MPa)
	b (mm)	h (mm)	t_f (mm)	t_w (mm)	d_w/t_w		
Initial study set							
IS1-1-690	250	231	18	10	16.7	$10^{-5}h_w$	690
IS1-1-960							960
IS2-2-690	250	511	18	10	44.7	$10^{-5}h_w$	690
IS2-2-960							960
Series WT							
WT1-1-690	IS1-1-690						690
WT1-1-960	IS1-1-960						960
WT2-1-690	250	231	18	8	20.8	$10^{-5}h_w$	690
WT2-1-960							960
WT3-1-690	250	231	18	6	27.8	$10^{-5}h_w$	690
WT3-1-960							960
WT4-1-690	250	231	18	3	55.6	$10^{-5}h_w$	690
WT4-1-960							960
WT5-1-690	250	231	18	12	13.9	$10^{-5}h_w$	690
WT5-1-960							960
WT6-1-690	250	231	18	15	11.1	$10^{-5}h_w$	690
WT6-1-960							960
WT7-1-690	250	231	18	18	9.3	$10^{-5}h_w$	690
WT7-1-960							960
WT8-2-690	IS2-2-690						690
WT8-2-960	IS2-2-960						960
WT9-2-690	250	511	18	8	55.8	$10^{-5}h_w$	690
WT9-2-960							960
WT10-2-690	250	511	18	6	74.5	$10^{-5}h_w$	690
WT10-2-960							960
WT11-2-690	250	511	18	14	31.9	$10^{-5}h_w$	690
WT11-2-960							960
WT12-2-690	250	511	18	18	24.8	$10^{-5}h_w$	690
WT12-2-960							960
Series FT							
FT1-1-690	IS1-1-690						690
FT1-1-960	IS1-1-960						960
FT2-1-690	250	231	15	10	17.3	$10^{-5}h_w$	690
FT2-1-960							960
FT3-1-690	250	231	21	10	16.1	$10^{-5}h_w$	690
FT3-1-960							960
FT4-1-690	WS2-1-690						690
FT4-1-960	WS2-1-960						960
FT5-1-690	250	231	15	8	21.6	$10^{-5}h_w$	690
FT5-1-960							960
FT6-1-690	250	231	21	8	20.1	$10^{-5}h_w$	690
FT6-1-960							960

Table 1. Continued...

Test	Geometric properties					Out-of--flatness	$f_{y,nom}$
	b (mm)	h (mm)	t_f (mm)	t_w (mm)	d_w/t_w		(MPa)
Series WT							
FT7-1-690			WS6-1-690				690
FT7-1-960			WS6-1-960				960
FT8-1-690	250	231	15	15	11.5	$10^{-5}h_w$	690
FT8-1-960							960
FT9-1-690	250	231	21	15	10.7	$10^{-5}h_w$	690
FT9-1-960							960
FT10-2-690			IS2-2-690				690
FT10-2-960			IS2-2-960				960
FT11-2-690	250	511	15	10	45.3	$10^{-5}h_w$	690
FT11-2-960							960
FT12-2-690	250	511	21	10	44.1	$10^{-5}h_w$	690
FT12-2-960							960
Series WI							
WI1-1-690			IS1-1-690				690
WI1-1-960			IS1-1-960				960
WI2-1-690	250	231	18	10	16.7	$10^{-3}h_w$	690
WI2-1-960							960
WI3-1-690	250	231	18	10	16.7	$10^{-2}h_w$	690
WI3-1-960							960
WI4-1-690			WS2-1-690				690
WI4-1-960			WS2-1-960				960
WI5-1-690	250	231	18	8	20.8	$10^{-3}h_w$	690
WI5-1-960							960
WI6-1-690	250	231	18	8	20.8	$10^{-2}h_w$	690
WI6-1-960							960
WI7-1-690			IS2-2-690				690
WI7-1-960			IS2-2-960				960
WI8-2-690	250	511	18	10	44.7	$10^{-3}h_w$	690
WI8-2-960							960
WI9-2-690	250	511	18	10	44.7	$10^{-2}h_w$	690
WI9-2-960							960

4.1 Description of the model

The FE modelling of the behaviour of a column web under transverse compression requires an adequate representation of the column geometry, the material constitutive laws, boundary and load conditions. The model has to reflect global structural behaviour. Such behaviour is three-dimensional in nature and is well captured by shell elements. This type of elements is suitable for bending- and membrane-dominated problems in relatively thin structures. Thick shells are also able to accommodate transverse shear deformations. Considerable savings in computer time and analysis are achieved because

only the mid-surface of the structure is modelled.

Additionally, the FE model must reproduce the relevant failure mode. Since out-of-plane buckling deformations do not occur in perfectly flat plates under in-plane loading conditions, a relatively small initial out-of-plane distortion of $10^{-5}h_w$ was introduced (h_w is the depth of the column web). The shape of initial deformations are based on the specifications for welded profiles adopted in EN 1090-2 (CEN 2008) - Fig. 3. According to this norm, allowable initial variations of flatness of webs in welded profiles are much greater than this value.

In order to model a more realistic strength behaviour, the flange-to-web welds were included in the FE analysis, as they are considered to be an important factor in terms of resistance predictions. The cross-section details and the model assumptions regarding the welds connecting the flange and the web are shown schematically in Fig. 4.

4.1.1 Mesh description

The simply supported I-column was generated with QTS4 three-dimensional four-node thick shell elements, available in the element library of the FE code LUSAS (FEA 2006). These elements belong to a family of serendipity isoparametric elements. The elements have six degrees-of-freedom per node (u, v, w, θ_x, θ_y and θ_z) relating to global axes and are numerically integrated (five-layer through-thickness integration rule). The element formulation is based on an assumed strain field to define transverse shear. This incompatible strain field prevents locking of the element when it is thin and is essential for a good performance in bending for this lower order element (FEA 2006). This family of thick shell elements also offers a consistent formulation of tangent stiffness which makes them particularly effective in geometric nonlinear applications (FEA 2006).

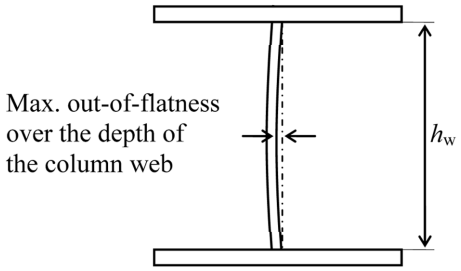

Fig. 3 Shape of initial deformations of the web

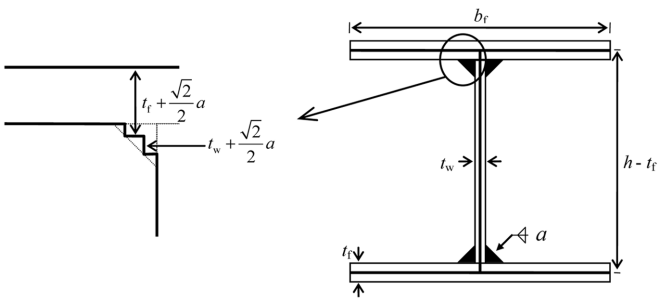

Fig. 4 Modelling of the flange-to-web weld

The kinematic description of these elements in nonlinear geometrical analysis is based on the total Lagrangian formulation that accounts for large displacements and small strains. Stresses and strains are output in terms of the "second Piola-Kirchoff stresses" and "Green-Lagrange strains", with reference to the undeformed configuration (FEA 2006). The correct elementation of the column web is naturally of the utmost importance in FE modelling. The FE mesh must be sufficiently refined to reproduce accurate results, but the number of elements has to be kept as small as possible in order to limit the processing time needed for the analysis.

A fine mesh discretization of the I-column web near the load application point is required to capture the development of plasticity and instability phenomena. The number of elements exterior to this zone is greatly reduced as it does not influence the overall behaviour. The mesh density is chosen in order to avoid severe distortion of elements. Common practice suggests a maximum element aspect ratio of 6~7. It was found that the FE mesh depicted in Fig. 5 complies with the requirements for a reliable simulation and satisfies the convergence requirements.

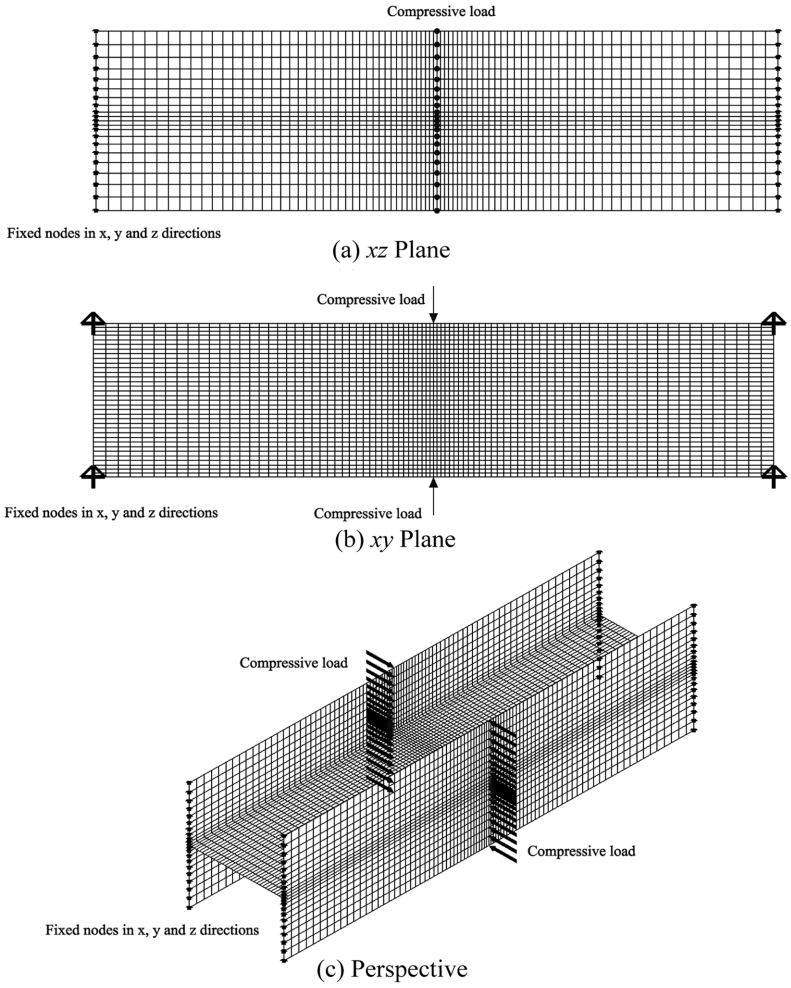

Fig. 5 Finite element mesh (*e.g.*, IS1-1)

4.1.2 Material properties

The elastoplastic material response is taken into account through dissociation of the elastic and plastic deformations. Plasticity is modelled with strain hardening. The plasticity formulations are based on three fundamental concepts (Bathe and Wilson 1976): (i) a yield condition to specify the onset of plastic deformation, (ii) a flow rule to define the plastic straining and (iii) a hardening rule to define the evolution of the yield surface with plastic straining. The yield condition is defined under the Von Mises yield criterion. An associated flow rule defines the direction plastic strain vector. The constitutive model is integrated by means of the explicit forward Euler algorithm (Owen and Hinton 1980).

In order for an element formulation to be applicable to a specific response prediction, both kinematic and constitutive descriptions must be appropriate (Bathe 1982). In a materially nonlinear-only analysis, the configuration and volume of the body under consideration are constant. In this type of analysis, both displacements and rotations are assumed to be infinitesimally small. In a large displacement and strain elastoplastic analysis, the configuration and volume of the body do not remain constant. The Lagrangian formulation includes the kinematic nonlinear effects due to large displacements and strains, but whether the large strain behaviour is modelled accurately depends on the constitutive relations specified. This requires the use of a true stress-logarithmic (or natural) strain measure ($\sigma_n - \varepsilon_n$) for the definition of the uniaxial material response, instead of the classic engineering constitutive law ($\sigma - \varepsilon$). These quantities are defined with respect to the current length and cross-sectional area of the coupon and are related to the engineering values, σ and ε, by means of the following relationships

$$\sigma_n = \sigma(1 + \varepsilon) \qquad \varepsilon_n = \ln(1 + \varepsilon) \tag{4}$$

The full actual stress-strain of the materials is reproduced with a piecewise linear model, as shown in Fig. 6 for both S690 and S960 beam web and flanges. The material properties are taken from previous work from the authors (Girão Coelho *et al*. 2009). The mechanical characteristics of the material are given in Table 2. Values are given for the following characteristics: Young modulus E, strain hardening modulus E_{st}, static yield and tensile stresses f_y and f_u, strain at the strain hardening point ε_{st}, uniform strain ε_{uni} and strain at rupture load ε_f.

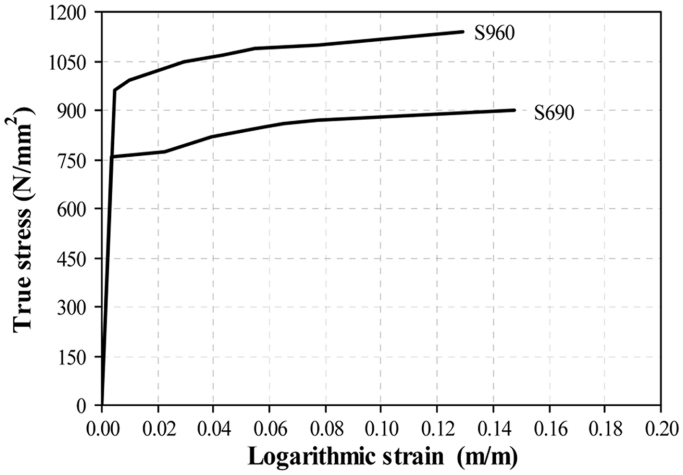

Fig. 6 Stress-strain behaviour (column web).

Table 2 Mechanical properties

Steel grade	S690		S960	
	Web (t_w = 10 mm)	Flange (t_f = 18 mm)	Web (t_w = 10 mm)	Flange (t_f = 18 mm)
E (N/mm^2)	208400	212667	209250	205780
E_{st} (N/mm^2)	1426	1547	4850	3533
f_y (N/mm^2)	756	755	958	969
f_u (N/mm^2)	807	803	1028	1026
ε_{st}	2.28×10^{-2}	1.60×10^{-2}	0.72×10^{-2}	0.70×10^{-2}
ε_{uni}	6.73×10^{-2}	6.94×10^{-2}	5.62×10^{-2}	5.41×10^{-2}
ε_f	15.91×10^{-2}	18.06×10^{-2}	13.78×10^{-2}	16.14×10^{-2}

4.1.3 Boundary and load conditions

Appropriate boundary conditions that are consistent with the actual column restraints are applied. At the column ends, the nodes in the flange are restrained against horizontal and vertical displacements (Fig. 5).

Load is applied to the specimen in a displacement-control fashion which enforces a better conditioning of the tangent stiffness matrix when compared to the classical load-control procedure.

4.1.4 Solution procedure

To determine the structural response of the nonlinear problem an implicit solution strategy is employed, which is suitable for problems involving smooth nonlinear analyses. A load stepping routine is thus used. There was no restriction on the magnitude of the load step as the procedure is unconditionally stable. The increment size follows from accuracy and convergence criteria. Within each increment, the equilibrium equations are solved by means of the Newton-Raphson method, which is stable and converges quadratically. In the Newton-Raphson method, for each load step, the residuals are eliminated by an iterative scheme. In each iteration the load level remains constant and the structure is analysed with a redefined tangent stiffness matrix. The accuracy of the solution is measured by means of appropriate convergence criteria. The following criteria were used (FEA 2006): (i) Euclidean displacement norm = 3.0, (ii) Euclidean incremental norm = 3.0 and (iii) work norm = 0.05.

The nonlinear iteration procedure is set to be terminated when the stiffness matrix becomes almost singular. This happens when a limit point is approached, *i.e.* in the vicinity of the maximum resistance. It must be emphasized that the studies presented in this paper do not address the issue of deformation capacity. This work is mainly concerned with the validation of current design rules of the EN 1993 to include the compression zone of column webs made from high-strength steel. Therefore, only the elastic behaviour and the strength properties are evaluated.

4.2 Model validation

A number of experimental tests from the literature were reproduced in this investigation for the purpose of verifying the accuracy of the FE prediction model outlined previously. Shown in Table 3 are comparisons between numerical and experimental results for several specimens tested by Aribert *et al*. (series M and MH) (1990) and by Kuhlmann (1999) and Kuhlmann and Kühnemund (2000b) (A3). The numerical analysis is based on geometrical and mechanical characteristics represented in the above references. Included in the study are the strength characteristics. The table shows that the numerical predictions for ultimate resistance are in good agreement with the experimental results.

Table 3 Details of previous tests on the web under compression

Test	Section	Geometric characteristics [mm]					Steel grade	Mechanical properties [MPa]				Strength	
		h	b_f	t_w	t_f	r		$f_{y,f}$	$f_{u,f}$	$f_{y,w}$	$f_{u,w}$	$F_{max,exp}$	$F_{max,num}$
M1	IPE140	141.9	74.2	5.1	6.4	7.8	S235	282	399	303	416	175	163
M2	HEA260	255.3	259.8	7.8	11.8	23.8	S235	300	456	335	459	608	593
M3	IPE220	220.0	111.4	6.2	8.6	13.1	S235	305	463	284	468	300	270
M4	IPE360	359.5	170.8	8.3	12.5	16.8	S235	273	423	326	435	530	542
MH1	HEA140	135.5	140.2	5.7	8.8	11.8	S460	477	571	484	578	365	348
MH2	HEA160	154.3	160.6	6.7	10.0	13.4	S460	477	589	481	608	530	506
MH4	HEA200	195.9	203.6	7.7	11.2	18.2	S460	512	613	542	640	760	754
MH8	IPE240	238.6	120.2	6.1	10.6	14.3	S460	488	584	566	671	454	457
A3	HEA240	230.0	240.0	7.5	12.0	21.0	S235	287	512	286	524	502	534

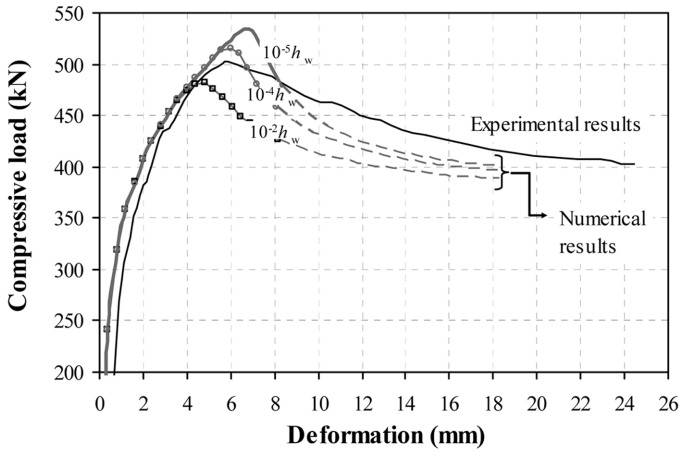

Fig. 7 Load-deformation response for specimen A3

Fig. 7 compares the experimental and numerical force-deformation curves for specimen A3. Only the portion of the curves for $F_{c,wc} > 200$ kN is shown to increase the resolution of the plots. A close examination of the figure shows that although the resistance is well represented, the initial stiffness is higher than that experimentally obtained, possibly because a number of phenomena from the experiments, such as imperfection in the test setup, lack of fit and initial slippery, were not included in the FE analysis. Another reason for the differences in results is the modelling of the stress-strain curve. The actual full stress-strain curve is not reported. It was then decided to adopt a piecewise stress-strain relationship based on the available mechanical properties, with a bilinear model for strain-hardening, as proposed by Gioncu and Mazzolani (2002).

Some discrepancy is also observed in the final stage of the curve, where failure is due to postyield web buckling. Although the LUSAS software is capable of handling postyield buckling phenomenon, the results are particularly sensitive to the amplitude of the initial web imperfection (out-of-flatness). In this particular study of specimen A3, a web out-of-plane distortion of $10^{-5}h_w$, $10^{-4}h_w$ and $10^{-2}h_w$ has been assumed. Differences in the ultimate response are quite clear in Fig. 7. The maximum strength

predictions are as follows: 534 kN (value in Table 3), 516 kN and 482 kN for the above web out-of-flatness values, respectively.

This preliminary study shows that the quantitative and qualitative response of the numerical simulations with respect to the strength properties correspond to those of the experiments. This underlines the accuracy of the FE model.

Table 4 Summary of FE results (Continued)

Test	Strength			Initial stiffness	Failure mode	
	$F_{c,wc,Rp}$ (kN)	$F_{c,wc,u}$ (kN)	Ratio	$k_{c,wc,e}$ (kN/mm)	"Pseudo-plastic" conditions	Ultimate conditions
Initial study set						
IS1-1-690	1080	1564	1.45	1399.8	Crushing	
IS2-2-690	1379	1476	1.07	1299.5	Buckling	
IS1-1-960	1510	1930	1.28	1658.5	Crushing	
IS2-2-960	1482	1722	1.16	1343.9	Buckling	
Series WT						
WT1-1-690	1080	1564	1.45	1399.8	Crushing	
WT2-1-690	810	1266	1.56	1564.4	Crushing	Buckling
WT3-1-690	710	963	1.36	1357.9	Crushing	Buckling
WT4-1-690	360	420	1.17	840.8	Buckling	
WT5-1-690	1280	1741	1.36	1580.1	Crushing	
WT6-1-690	1500	1984	1.32	1830.9	Crushing	
WT7-1-690	1665	2210	1.33	2058.2	Crushing	
WT8-2-690	1379	1476	1.07	1299.5	Buckling	
WT9-2-690	847	1042	1.23	1132.1	Buckling	
WT10-2-690	688	1005	1.46	887.7	Buckling	
WT11-2-690	1615	2013	1.25	1717.2	Crushing	
WT12-2-690	1915	2334	1.22	2052.7	Crushing	
WT1-1-960	1510	1930	1.28	1658.5	Crushing	
WT2-1-960	1075	1416	1.32	1638.3	Crushing	Buckling
WT3-1-960	877	1158	1.32	1361.3	Buckling	
WT4-1-960	455	611	1.34	796.2	Buckling	
WT5-1-960	1625	2157	1.33	2068.7	Crushing	
WT6-1-960	1800	2469	1.37	3594.9	Crushing	
WT7-1-960	2100	2758	1.31	2853.6	Crushing	
WT8-2-960	1482	1722	1.16	1343.9	Buckling	
WT9-2-960	1245	1615	1.30	1034.9	Buckling	
WT10-2-960	800	1182	1.48	902.6	Buckling	
WT11-2-960	2038	2533	1.24	1746.1	Crushing	
WT12-2-960	2410	2944	1.22	2094.4	Crushing	

Table 4 Continued...

Test	Strength			Initial stiffness	Failure mode	
	$F_{c,wc,Rp}$ (kN)	$F_{c,wc,u}$ (kN)	Ratio	$k_{c,wc,e}$ (kN/mm)	"Pseudo-plastic" conditions	Ultimate conditions
Series FT						
FT1-1-690	1080	1564	1.45	1399.8	Crushing	
FT2-1-690	970	1320	1.36	1608.2	Crushing	
FT3-1-690	1260	1757	1.39	1889.6	Crushing	Buckling
FT4-1-690	810	1266	1.56	1564.4	Crushing	Buckling
FT5-1-690	770	1123	1.46	1379.1	Crushing	Buckling
FT6-1-690	1025	1275	1.24	1751.9	Crushing	Buckling
FT7-1-690	1500	1984	1.32	1830.9	Crushing	
FT8-1-690	1295	1675	1.29	2101.7	Crushing	
FT9-1-690	1720	2296	1.34	2655.1	Crushing	
FT10-2-690	1379	1476	1.07	1299.5	Buckling	
FT11-2-690	1276	1363	1.07	1227.2	Buckling	
FT12-2-690	1460	1563	1.07	1427.0	Buckling	
FT1-1-960	1510	1930	1.28	1658.5	Crushing	
FT2-1-960	1250	1638	1.31	1697.0	Crushing	
FT3-1-960	1522	2109	1.39	2044.8	Crushing	Buckling
FT4-1-960	1075	1416	1.32	1638.3	Crushing	Buckling
FT5-1-960	990	1328	1.34	1469.9	Crushing	Buckling
FT6-1-960	1114	1515	1.36	1827.8	Crushing	Buckling
FT7-1-960	1800	2469	1.37	3594.9	Crushing	
FT8-1-960	1740	2094	1.20	2221.2	Crushing	
FT9-1-960	2130	2840	1.33	2746.3	Crushing	
FT10-2-960	1482	1722	1.16	1343.9	Buckling	
FT11-2-960	1415	1595	1.13	1254.9	Buckling	
FT12-2-960	1563	1819	1.16	1454.7	Buckling	
Series WI						
WI1-1-690	1080	1564	1.45	1399.8	Crushing	
WI2-1-690	1086	1503	1.38	1400.2	Crushing	Buckling
WI3-1-690	1060	1295	1.22	1366.2	Combined mechanism	
WI4-1-690	810	1266	1.56	1564.4	Crushing	Buckling
WI5-1-690	820	1112	1.36	1563.4	Crushing	Buckling
WI6-1-690	800	946	1.18	1477.3	Buckling	
WI7-2-690	1379	1476	1.07	1299.5	Buckling	
WI8-2-690	1175	1460	1.24	1297.0	Buckling	
WI9-2-690	1025	1371	1.34	1139.0	Buckling	
WI1-1-960	1510	1930	1.28	1658.5	Crushing	
WI2-1-960	1490	1812	1.22	1658.0	Combined mechanism	
WI3-1-960	1340	1572	1.17	1606.9	Combined mechanism	
WI4-1-960	1075	1416	1.32	1638.3	Crushing	Buckling
WI5-1-960	1070	1316	1.23	1636.0	Combined mechanism	
WI6-1-960	925	1140	1.23	1547.0	Buckling	
WI7-2-960	1482	1722	1.16	1343.9	Buckling	
WI8-2-960	1445	1709	1.18	1341.1	Buckling	
WI9-2-960	1270	1598	1.26	1163.3	Buckling	

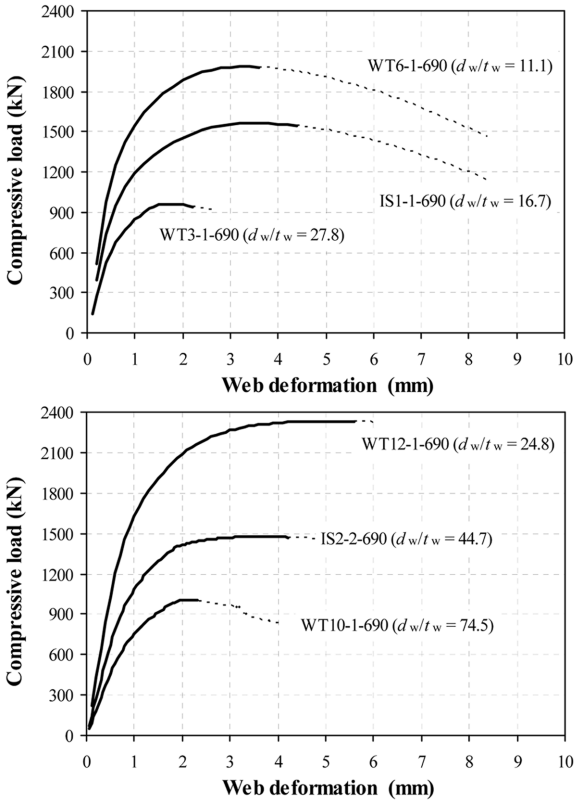

Fig. 8 Load-deformation characteristics: effect of web thickness

5. Analysis results

Table 4 summarizes the strength and initial stiffness $k_{c,wc,e}$ results from all the parametric studies. The "pseudo-plastic" resistance level $F_{c,wc,Rp}$, the maximum compressive strength $F_{c,wc,u}$ and the ratio $F_{c,wc,u}/F_{c,wc,Rp}$ are given in the table. The term "pseudo-plastic" is adopted from Jaspart (1997) and is used below because in some cases the instability phenomenon precedes full plasticity. Figs. 8 and 10-12 plot the force-deformation curves of some models. Each of the figures focuses on illustrating the effects of several sets of parameters. These are discussed in the following subsections from a strength point of view and governing failure mode.

5.1 Effects of the web thickness on compressive strength

The effects of the web thickness on the resistance of column webs subjected to transverse compression are examined below. First, the two initial study sets are analysed. These models are then analysed with varying web thickness (series WT – Table 1). The column section depth was fixed at 231 mm and 511 mm. The web thickness has been varied from 3 mm ($t_f / t_w = 6$) to 18 mm ($t_f / t_w = 1$). The web slenderness d_w / t_w varied from 11.1 to 74.5. Of the cross-section based variables, the web thickness parameter is naturally expected to influence the strength capacity significantly.

Fig. 8 shows the ultimate strength behaviour of the various tests. Results are summarized and compared

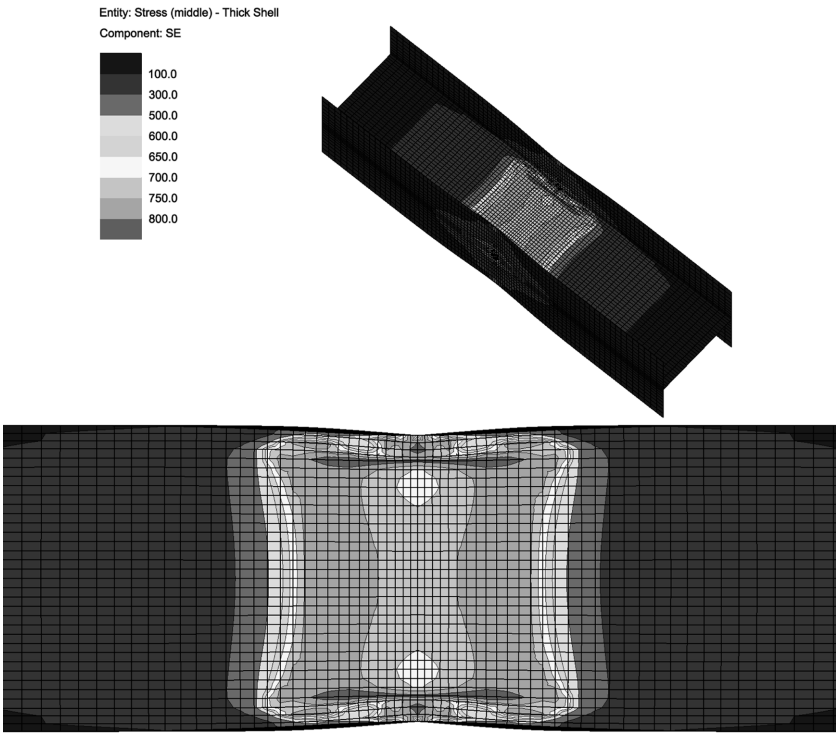

a) IS1-1-690

Fig. 9 Failure modes of column web due to crushing and buckling (deformed mesh amplification factor = 3.0) (Continued)

in Table 4. The following observations are made

- strength capacity of thicker webs is higher;
- ductility characteristics improve as web slenderness decreases;
- compact webs typically fail by crushing; as slenderness increases, inelastic buckling behaviour becomes dominant and slender webs eventually fail by excessive out-of-plane deflections (Fig. 9);
- strength capacities always exceed the "pseudo-plastic" capacity, even in the case of extremely slender webs.

This indicates that there is a large margin of reserve post-yield (or post-buckling) strength in the column web.

5.2 Effects of flange thickness on compressive strength

Flange thickness values of 15 mm, 18 mm and 21 mm are considered in this work. The contribution of the flanges to the resisting capacity is particularly significant for webs with lower web slenderness ratios d_w / t_w, as can be seen from Table 4 and Fig. 10. For $d_w / t_w \approx 17$ (Fig. 10a), the maximum capacity is improved by about 12% by changing the flange thickness from 18 mm to 21 mm (~17%), although the unloading from the peak force becomes very abrupt. However, for $d_w/t_w \approx 45$ (Fig. 10b), the differences in strength are much smaller. The post-peak load-deformation characteristics are significantly affected by the flange thickness. The use of thinner flanges tends to result in a "plateau" in the response,

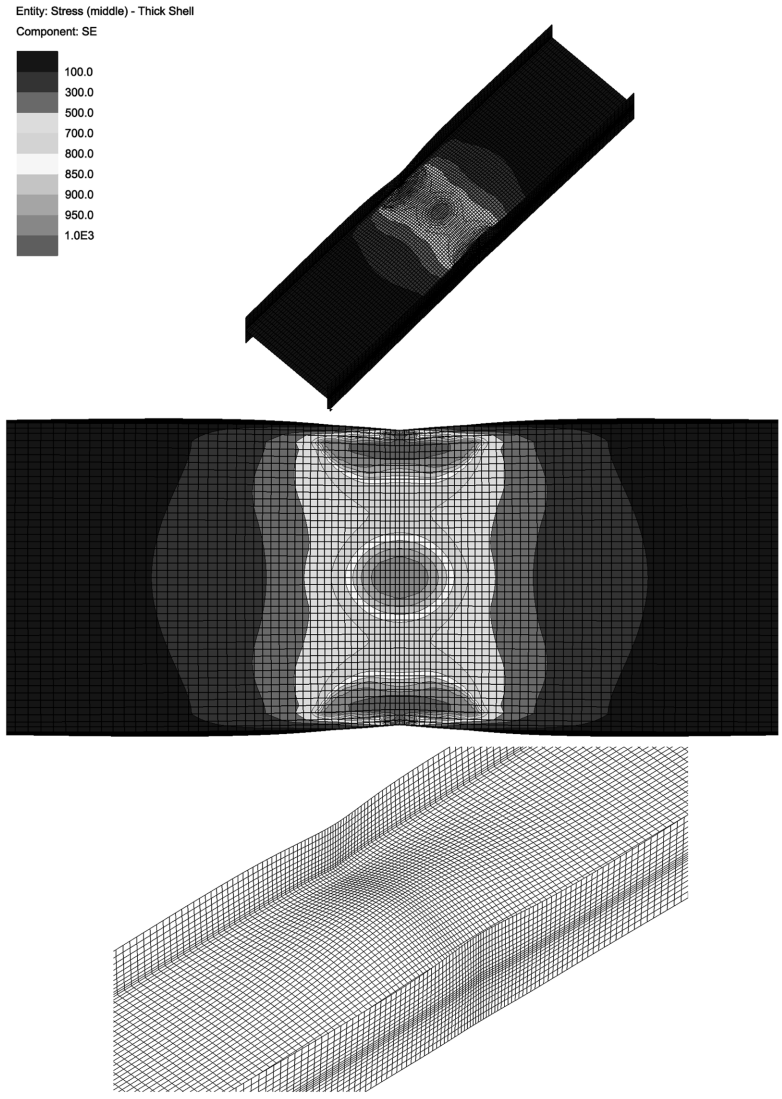

b) IS2-2-960

Fig. 9 Failure modes of column web due to crushing, buckling and inelastic buckling (deformed mesh amplification factor = 3.0) (Continued)

whereas for thicker flanges the post-peak strength rapidly decreases.

5.3 Effects of large initial deformations on compressive strength

The design equations for evaluation of the compressive strength of column webs have been formulated for webs with relatively small initial deformations. Previous models assumed an initial out-of-flatness of $10^{-5}h_w$. According to EN 1090-2 (CEN 2008), variations from flatness can be as high as $10^{-2}h_w$. To investigate the effects of larger initial deformations on compressive strength, an initial out-of-plane

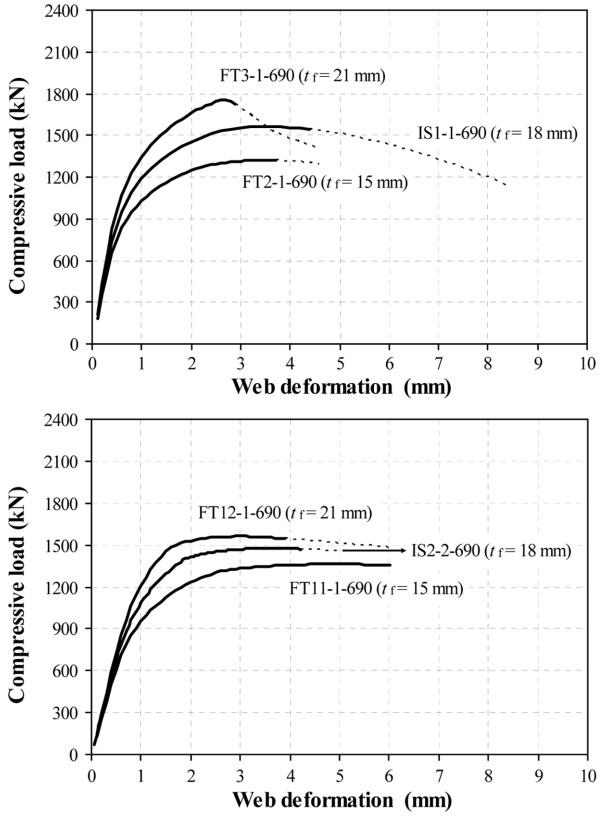

Fig. 10 Load-deformation characteristics: effect of flange thickness

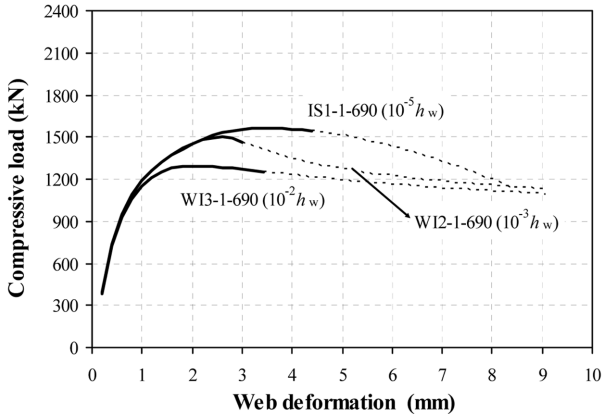

Fig. 11 Load-deformation characteristics: effect of web out-of-flatness

distortion of $10^{-3}h_w$ and $10^{-2}h_w$ was introduced into the column web (Table 1, series WI).

Fig. 11 and Table 4 compare the ultimate strength behaviour and the failure mechanisms of column webs with different initial out-of-flatness values. Comparisons demonstrate that

· reduction of ("pseudo-plastic" and ultimate) strength due to larger out-of-flatness values is quite

significant, particularly for webs with lower web slenderness ratios d_w/t_w;
· imperfection-induced transition from crushing to buckling failure mode results in reductions of ultimate resistance; in fact, if initial larger deformations are present in the column web, the failure mode involves buckling, even in the case of stockier webs, because a considerable out-of-plane bending action is likely to take place; this leads to a strength reduction that can be particularly significant (*e.g.*, WI6-1-690 and WI4-1-690, reduction of 25% in compressive strength).

5.4 Effects of material mechanical characteristics on compressive strength

Examination of the FE analysis data in Table 4 and Fig. 12 reveals that
· compressive strength is always higher when higher steel grades are employed;
· observed collapse behaviour is not greatly influenced by the steel grade;
· the ratio between ultimate strength values for specimens made from S960 and S690 is identical to the ratio between the actual yield stress values of both grades (1.27) when the failure mode involves a bearing mechanism and is consistently lower (~1.17) when buckling is present. These ratios clearly indicate that the column web underwent large inelastic deformations, due to material strain hardening or buckling (or a combination of both) before the maximum strength was reached.

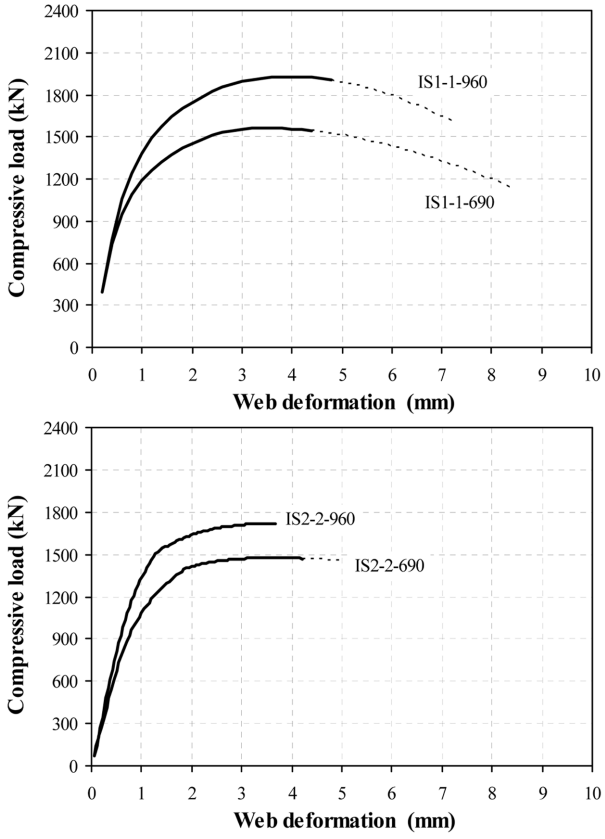

Fig. 12 Load-deformation characteristics: effect of material strength properties

6. Conclusions

The current EN 1993 design criteria do not permit the use of the plastic capacity and inelastic procedures for joint components (column webs in transverse compression, in particular) made from high-strength steels because few research studies have been carried out to demonstrate that column webs provide adequate force-deformation behaviour. In spite of the limited number of simulation studies examined, the FE results provide some support for questioning the need for these restrictions when designing high-strength steel column webs in transverse compression. Based on the results obtained from

Table 5 Comparisons with EN 1993-1-8 predictions (Continued)

Test	Strength predictions						Elastic stiffness predictions		
	EN 1993-1-8			Numerical results		Ratio to FE results	EN 1993-1-8	Numerical results	Ratio to FE results
	$F_{c,wc,R}$ (kN)	$F^{*}_{c,wc,R}$ (kN)	Failure mode	$F_{c,wc,Rp}$ (kN)	Failure mode		$k_{c,wc,e}$ (kN/mm)	$k_{c,wc,e}$ (kN/mm)	
Initial study set									
IS1-1-690	1215	1006	Buckling	1080	Crushing	0.93	1406.3	1399.8	1.00
IS2-2-690	1215	690	Buckling	1379	Buckling	0.50	524.8	1299.5	0.40
IS1-1-960	1540	1174	Buckling	1510	Crushing	0.78	1412.0	1658.5	0.85
IS2-2-960	1540	793	Buckling	1482	Buckling	0.54	527.0	1343.9	0.39
Series WT									
WT1-1-690	1215	1006	Buckling	1080	Crushing	0.93	1406.3	1399.8	1.00
WT2-1-690	972	684	Buckling	810	Crushing	0.84	1125.0	1564.4	0.72
WT3-1-690	729	408	Buckling	710	Crushing	0.57	843.8	1357.9	0.62
WT4-1-690	364	110	Buckling	360	Buckling	0.31	421.9	840.8	0.50
WT5-1-690	1458	1357	Buckling	1280	Crushing	1.06	1687.5	1580.1	1.07
WT6-1-690	1822	1822	Crushing	1500	Crushing	1.21	2109.4	1830.9	1.15
WT7-1-690	2187	2187	Crushing	1665	Crushing	1.31	2531.3	2058.2	1.23
WT8-2-690	1215	690	Buckling	1379	Buckling	0.50	524.8	1299.5	0.40
WT9-2-690	972	456	Buckling	847	Buckling	0.54	419.9	1132.1	0.37
WT10-2-690	729	265	Buckling	688	Buckling	0.39	314.9	887.7	0.35
WT11-2-690	1701	1259	Buckling	1615	Crushing	0.78	734.7	1717.2	0.43
WT12-2-690	2187	1928	Buckling	1915	Crushing	1.01	944.7	2052.7	0.46
WT1-1-960	1540	1174	Buckling	1510	Crushing	0.78	1412.0	1658.5	0.85
WT2-1-960	1232	792	Buckling	1075	Crushing	0.74	1129.6	1638.3	0.69
WT3-1-960	924	468	Buckling	877	Buckling	0.53	847.2	1361.3	0.62
WT4-1-960	462	126	Buckling	455	Buckling	0.28	423.6	796.2	0.53
WT5-1-960	1848	1598	Buckling	1625	Crushing	0.98	1694.4	2068.7	0.82
WT6-1-960	2309	2309	Crushing	1800	Crushing	1.28	2118.0	3594.9	0.59
WT7-1-960	2771	2771	Crushing	2100	Crushing	1.32	2541.6	2853.6	0.89
WT8-2-960	1540	793	Buckling	1482	Buckling	0.54	527.0	1343.9	0.39
WT9-2-960	1232	522	Buckling	1245	Buckling	0.42	421.6	1034.9	0.41
WT10-2-960	924	302	Buckling	800	Buckling	0.38	316.2	902.6	0.35
WT11-2-960	2155	1460	Buckling	2038	Crushing	0.72	737.7	1746.1	0.42
WT12-2-960	2771	2260	Buckling	2410	Crushing	0.94	948.5	2094.4	0.45

Table 5. Continued...

Test	Strength predictions								
	EN 1993-1-8			Numerical results		Ratio to FE results	EN 1993-1-8	Numerical results	Ratio to FE results
	$F_{c,wc,R}$ (kN)	$F^*_{c,wc,R}$ (kN)	Failure mode	$F_{c,wc,Rp}$ (kN)	Failure mode		$k_{c,wc,e}$ (kN/mm)	$k_{c,wc,e}$ (kN/mm)	
Series FT									
FT1-1-690	1215	1006	Buckling	1080	Crushing	0.93	1406.3	1399.8	1.00
FT2-1-690	1102	931	Buckling	970	Crushing	0.96	1230.7	1608.2	0.77
FT3-1-690	1328	1080	Buckling	1260	Crushing	0.86	1594.9	1889.6	0.84
FT4-1-690	972	684	Buckling	810	Crushing	0.84	1125.0	1564.4	0.72
FT5-1-690	881	635	Buckling	770	Crushing	0.82	984.6	1379.1	0.71
FT6-1-690	1063	733	Buckling	1025	Crushing	0.72	1275.9	1751.9	0.73
FT7-1-690	1822	1822	Crushing	1500	Crushing	1.21	2109.4	1830.9	1.15
FT8-2-690	1652	1652	Crushing	1295	Crushing	1.28	1846.1	2101.7	0.88
FT9-2-690	1993	1993	Crushing	1720	Crushing	1.16	2392.4	2655.1	0.90
FT10-2-690	1215	690	Buckling	1379	Buckling	0.50	524.8	1299.5	0.40
FT11-2-690	1102	647	Buckling	1276	Buckling	0.51	469.5	1227.2	0.38
FT12-2-690	1328	731	Buckling	1460	Buckling	0.50	581.6	1427.0	0.41
FT1-1-960	1540	1174	Buckling	1510	Crushing	0.78	1412.0	1658.5	0.85
FT2-1-960	1396	1088	Buckling	1250	Crushing	0.87	1235.7	1697.0	0.73
FT3-1-960	1683	1259	Buckling	1522	Crushing	0.83	1601.4	2044.8	0.78
FT4-1-960	1232	792	Buckling	1075	Crushing	0.74	1129.6	1638.3	0.69
FT5-1-960	1117	736	Buckling	990	Crushing	0.74	988.6	1469.9	0.67
FT6-1-960	1347	848	Buckling	1114	Crushing	0.76	1281.1	1827.8	0.70
FT7-1-960	2309	2309	Crushing	1800	Crushing	1.28	2118.0	3594.9	0.59
FT8-2-960	2094	2094	Crushing	1740	Crushing	1.20	1853.6	2221.2	0.83
FT9-2-960	2525	2525	Crushing	2130	Crushing	1.19	2402.1	2746.3	0.87
FT10-2-960	1540	793	Buckling	1482	Buckling	0.54	527.0	1343.9	0.39
FT11-2-960	1396	745	Buckling	1415	Buckling	0.53	471.4	1254.9	0.38
FT12-2-960	1683	839	Buckling	1563	Buckling	0.54	584.0	1454.7	0.40

the analyses presented herein, and recognizing that only 52 individual webs were analysed, the following conclusions are made: (i) typical webs exhibit inelastic buckling behaviour, (ii) collapse is characterized by excessive out-of-plane deflections due to buckling after plastic deformation of the web and (iii) the magnitude of plastic deformations mainly depends on the web slenderness and the steel grade.

Consequently, in this section, the results of the three dimensional FE analyses above are compared with the design provisions of EN 1993-1-8, neglecting the restrictions imposed on the steel grade. Table 5 summarizes the compressive strength and elastic stiffness predictions. Calculated design strengths, Eqs. (1) and (2), are based on the actual yield stress values and assume unitary partial safety coefficients γ_{M0} and γ_{M1}. The design elastic stiffness is computed from Eq. (3) and includes the Young modulus

$$k_{\mathrm{c,wc,e}} = \frac{0.7Eb_{\mathrm{eff,c,wc}}t_{\mathrm{wc}}}{d_{\mathrm{wc}}} \tag{5}$$

Given the tendency of the EN 1993-1-8 stiffness model to underpredict elastic stiffness, particularly for those specimens that fail by buckling, it is recommended to use a stiffness modification factor. The definition of such a factor naturally requires further work that will be carried out as future work of the authors.

In general, the ability of the strength Eqs. (1) and (2) to predict compressive strength is not very good (see Table 5). The high EN 1993-1-8 / FE ratios (1.16 – 1.32) require some explanation. The design equations were derived for common ratios t_f / t_w. In these specific cases, the flange and web thickness are similar and the above ratio is close to unity. This is not likely to occur in practical joints. The table also shows that the code model is producing very conservative results in predicting compressive strength associated with the buckling mode. Recall from Eq. (2) that the reduction factor ρ for plate buckling is based on the Winter formula (Appendix 1). This formula was derived for mild steel plates and requires a more extensive study to verify that it is generally applicable to high-strength steels. The writers are conducting additional research to understand the implications of this approach, with an emphasis on steel grades S690 and S960.

In conclusion, the information presented in this paper takes an important step in assessing the current EN 1993 design provisions with regard to high-strength steels. The design criteria are not realistic and should be modified to give an accurate assessment of the strength capacity. Some relevant issues related to the behaviour of high-strength steel joint webs in transverse compression still require further investigation, namely the influence of an axial force in the column.

Experimental tests and additional numerical simulations are being carried out by the authors as a follow-up study to this research. In addition, the authors attempt to set up sound design criteria regarding the requirements for deformation capacity and ductility of webs in transverse compression in order to establish confidence in the inelastic design of column webs made from high-strength steel. The use of the stress-modified critical strain (SMCS) criterion as proposed by Chi *et al*. (2006) seems a promising research tool to predict ductile fracture when the column is subjected to large-scale yielding due to transverse compression.

Appendix 1: Background to EN 1993-1-8 design rules for the column web in compression

Early studies on the column web in compression by Zoetemeijer (1980) and Witteveen *et al*. (1982) included a series of experimental tests. It was recommended that the connecting beam flange force should be distributed at a slope of 1 : 1 through the end plate (if present) and then on a 2.5 : 1 slope through the column flange and web. Design equations to check web crushing and web buckling were proposed. Aribert and co-workers also conducted numerous experimental tests and numerical analyses on column webs in double compression and evaluated results from several research projects. Their research has been restricted to considerations of strength. They recommended a lower bound solution for the failure load that caters for interaction between crushing and buckling of the web (Aribert *et al*. 1990). Work by Jaspart and co-workers further extended the resistance predictions and covered the elastic analysis to set up design rules for predicting the elastic stiffness.

Recently, extensive studies of component behaviour have been conducted in Stuttgart by Kuhlmann *et al*. (1999, 2000b, 2002) and in Salerno by De Mita *et al*. (2008). Their contribution has mainly concentrated on the characterization of the ultimate behaviour and the ductility of the web in compression.

The typical behaviour of a column web in compression is shown in Fig. A1.1. As shown in this figure, force-deformation behaviour may in general be broken into three regions: a quasi-linear elastic region followed by a post-yield range of much reduced stiffness and a softening unloading curve. At ultimate resistance $F_{c,wc,max}$ the column web attains a deformation denoted by $\Delta_{c,wc,max}$, which is often assumed as the deformation capacity. A more realistic approach to the definition of the deformation capacity $\Delta_{c,wc,u}$ of this component can be found in Kuhlmann and Kühnemund (2002): $\Delta_{c,wc,u}$ is the deformation at which the force deteriorates back to the plastic resistance $F_{c,wc,Rd}$ after reaching a force above $F_{c,wc,Rd}$ through plastic deformation (Fig. A1.1). The ductility is defined as the amount of a plastic rotation that can be sustained while maintaining a certain percentage of the ultimate resistance. The ductility properties reflect the extension of the plastic deformations and the margin of post-yield or post-buckling resistance Girão Coelho *et al*. (2007b, 2009, 2010).

A1.1 Resistance formulae: crushing capacity

The design crushing resistance of the column web in compression is given by

$$F_{c,\,wc,\,Rd} = \frac{\omega k_{wc} b_{eff,\,c,\,wc} t_{wc} f_{y,\,wc}}{\gamma_{M0}} \tag{A1.1}$$

Web failure of this type is treated as a stress problem. The code assumes that the stress is uniformly distributed along $b_{eff,c,wc}$, as shown in Fig. A1.2.

A1.1.1 Reduction factors

The column web is subjected to horizontal normal stresses σ_0 produced by the transverse compressive force transmitted by the flanges. σ_0 interacts with the shear stresses in the panel zone, τ, and the vertical normal stresses acting in the column, σ_v (see Fig. A1.2).

ω is a coefficient that accounts for $\sigma_0 - t$ interaction and is derived from application of the Von Mises yield criterion. The above stress values are readily computed as follows

$$\sigma_0 = \frac{F_c}{b_{eff,\,c,\,wc} t_{wc}} \qquad \tau = \xi \frac{\beta F_c}{A_{vc}} \tag{A1.2}$$

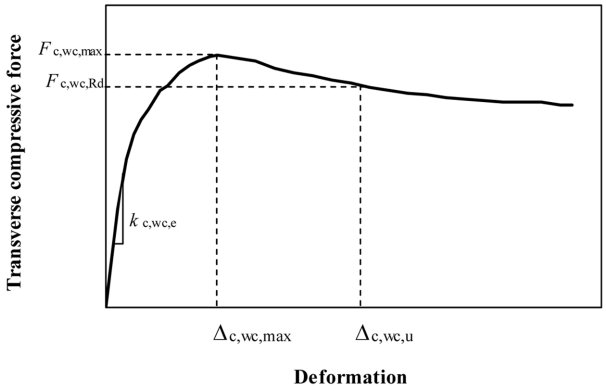

Fig. A1.1 Typical load-carrying behaviour of an unstiffened column web in compression

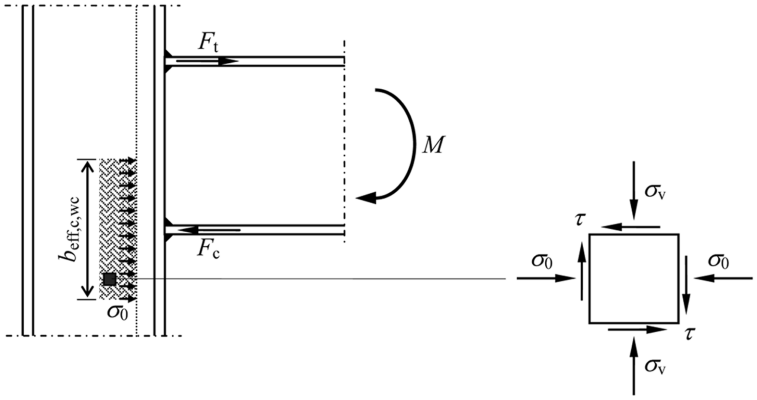

Fig. A1.2 Stresses in the compression zone of a beam-to-column joint

whereby A_{vc}: shear area of the column section; ξ: coefficient that accounts for the distribution of shear stresses in the web panel - Faella *et al*. (2000) suggest a value of 0.8; and β: transformation parameter related to the internal actions on the joint (CEN 2005b; Jaspart 1997). Conservative values for parameter β, neglecting the effect of the shear force in the column are suggested in EN 1993-1-8: (i) $\beta = 1$ in the case of one sided joints, (ii) $\beta = 2$ in the case of two sided joints with equal but unbalanced end bending moments and (iii) $\beta = 0$ in the case of two sided joints with balanced end bending moments. Bayo *et al*. (2006) recently initiated a research study on the evaluation of the β-factor. The authors demonstrate that the above limitations imposed on the β-factor may lead to substantial errors in the internal forces and moments.

According to the Von Mises yield criterion, local yielding of the column web under shear and compression occurs when the following condition is satisfied

$$f_{y,wc} = \sqrt{\sigma_0^2 + \tau^2} \tag{A1.3}$$

Substitution of σ_0 and τ for Eq. (A1.2) into the above equation gives

$$f_{y,wc} = \sqrt{\left(\frac{F_c}{b_{eff,c,wc}t_{wc}}\right)^2 + \left(\xi\frac{\beta F_c}{A_{vc}}\right)^2} \tag{A1.4}$$

Let $F_c = F_{c,wc,Rd}$ defined by Eq. (A1.1). Then by Eq. (A1.4)

$$\omega = \frac{1}{\sqrt{1 + 3\beta^2\xi^2\left(\frac{b_{eff,c,wc}t_{wc}}{A_{vc}}\right)^2}} \tag{A1.5}$$

Jaspart (1997) proposed a slightly different expression for the coefficient ω. This proposal was later included in EN 1993-1-8 that defines ω as follows

$$\text{For} \quad 0 \le \beta \le 0.5 \qquad \omega = 1$$

$$\text{For} \quad 0.5 < \beta \le 1 \qquad \omega = \omega_1 + 2(1-\beta)(1-\omega_1) \tag{A1.6}$$

$$\text{For} \quad 1 < \beta \leq 2 \qquad \omega = \omega_1 + (\beta - 1)(\omega_2 - \omega_1)$$

being

$$\omega_1 = \frac{1}{\sqrt{1 + 1.3\left(\frac{b_{\text{eff, c, wc}} t_{\text{wc}}}{A_{\text{vc}}}\right)^2}} \qquad \omega_2 = \frac{1}{\sqrt{1 + 5.2\left(\frac{b_{\text{eff, c, wc}} t_{\text{wc}}}{A_{\text{vc}}}\right)^2}} \tag{A1.7}$$

Regarding the coefficient k_{wc} that accounts for $\sigma_0 - \sigma_{\text{v}}$ interaction, Zoetemeijer (1980) proposed the following expression

$$k_{\text{wc}} = 1.25 - 0.5\frac{\sigma_{\text{v}}}{f_{\text{y, wc}}} \leq 1 \tag{A1.8}$$

EN 1993-1-8 adopts a more conservative relationship

$$\begin{aligned} &\text{For} \qquad \frac{\sigma_{\text{v}}}{f_{\text{y, wc}}} \leq 0.7 \qquad k_{\text{wc}} = 1 \\ &\text{For} \qquad \frac{\sigma_{\text{v}}}{f_{\text{y, wc}}} > 0.7 \qquad k_{\text{wc}} = 1.7 - \frac{\sigma_{\text{v}}}{f_{\text{y, wc}}} \end{aligned} \tag{A1.9}$$

A1.1.2 Effective width

Formulae for the effective width is given in EN 1993-1-8 as a result of research work carried out in the Delft University of Technology and TNO (Zoetemeijer 1980; Witteveen *et al*. 1982). An area of web providing resistance to crushing is calculated on the force dispersion length taken from Fig. A1.3. EN 1993-1-8 adopts the following expressions

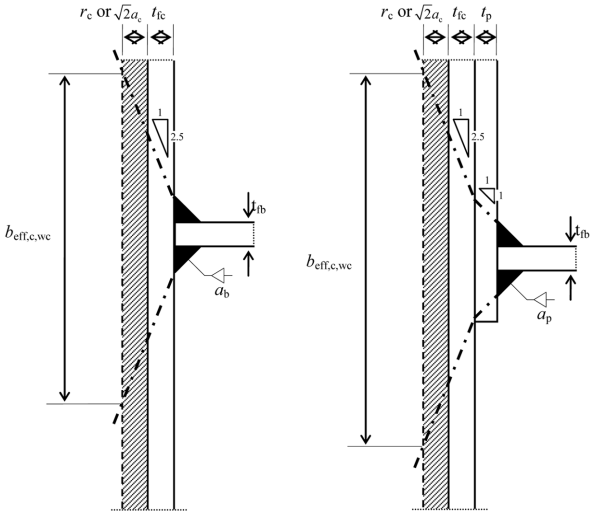

Fig. A1.3 Effective width for web crushing (a) welded connection and (b) end plate connection

$$\text{Welded connection} \qquad b_{\text{eff, c, wc}} = t_{\text{fb}} + 2\sqrt{2}a_{\text{b}} + 5(t_{\text{fc}} + s)$$

$$\text{Bolted connection} \qquad b_{\text{eff, c, wc}} = t_{\text{fb}} + 2\sqrt{2}a_{\text{q}} + 5(t_{\text{fc}} + s) + s_p \tag{A1.10}$$

whereby t_{fb} : beam flange thickness; t_{fc} : column flange thickness; a_{b} : throat thickness of the beam flange-to-column flange weld; a_{p} : throat thickness of the beam flange-to-end plate weld; s : for a rolled I-section, s is taken as the radius of the fillet of the web-to-flange connection of the column, r ; for a welded I-section, $s = \sqrt{2}a_{\text{c}}$, being a_{c} the throat thickness of the column web-to-flange weld; and s_{p}: length based on a 45° dispersion through the end plate ($t_{\text{p}} \le s_{\text{p}} \le 2t_{\text{p}}$).

A1.2 Resistance formulae: buckling capacity

The design buckling resistance of the column web in compression is given by

$$F^*_{\text{c, wc, Rd}} = \frac{\omega k_{\text{wc}} \rho b_{\text{eff, c, wc}} t_{\text{wc}} f_{\text{y, wc}}}{\gamma_{\text{M1}}} \le F_{\text{c, wc, Rd}} \tag{A1.11}$$

The reduction factor ρ is evaluated by means of the following expressions

$$\begin{aligned} &\text{For} \quad \overline{\lambda}_{\text{p}} \le 0.72 \qquad \rho = 1 \\ &\text{For} \quad \overline{\lambda}_{\text{p}} > 0.72 \qquad \rho = \left[\frac{1}{\overline{\lambda}_{\text{p}}}\left(1 - \frac{0.22}{\overline{\lambda}_{\text{p}}}\right)\right] \end{aligned} \tag{A1.12}$$

whereby the plate slenderness $\overline{\lambda}_{\text{p}}$ is given by

$$\overline{\lambda}_{\text{p}} = 0.932\sqrt{\frac{b_{\text{eff, c, wc}} d_{\text{wc}} f_{\text{y, wc}}}{E t_{\text{wc}}^2}} \tag{A1.13}$$

Eq. (A1.12) is based on the classical Winter formula (Galambos 1998). Winter used the "effective width", $b^*_{\text{eff, c, wc}}$, concept to reflect the loss of stiffness and redistribution of stresses after buckling of a plate. Essentially, this semiempirical method is based on the fact that much of the load is carried by the region of the plate in the close vicinity of the edges. For a plate simply supported along the edges, Winter proposed the following expression for effective width

$$b^*_{\text{eff, c, wc}} = b\sqrt{\frac{\sigma_c}{f_y}}\left(1 - 0.25\sqrt{\frac{\sigma_c}{f_y}}\right) \tag{A1.14}$$

that was later changed to

$$b^*_{\text{eff, c, wc}} = b\sqrt{\frac{\sigma_c}{f_y}}\left(1 - 0.22\sqrt{\frac{\sigma_c}{f_y}}\right) \tag{A1.15}$$

as a result of many tests and studies of postbuckling strength of steel plates. In the above expressions

the notation is as follows: b: actual plate width; and σ_c : elastic critical stress.

The slenderness function is defined by

$$\bar{\lambda} = \sqrt{\frac{f_y}{\sigma_c}} \tag{A1.16}$$

Then Eq. (A1.15) can be written as follows

$$b^*_{\text{eff, c, wc}} = b\frac{1}{\bar{\lambda}}\left(1 - 0.22\frac{1}{\bar{\lambda}}\right) \tag{A1.17}$$

or

$$b^*_{\text{eff, c, wc}} = b_{\text{eff, c, wc}}\rho \tag{A1.18}$$

from Eq. (A1.12) and assuming $b = b_{\text{eff,c,wc}}$. Note that $b^*_{\text{eff, c, wc}} = b_{\text{eff, c, wc}}$ for $\overline{\lambda_p} = 0.67$, *i.e.*, $\rho = 1$ and the crushing resistance governs the failure mode. EN 1993-1-8 specifies a coefficient of 0.72 instead.

The plate slenderness in the form of Eq. (A1.13) is based on the analysis of a simply supported long rectangular plate compressed by two equal and opposite transverse forces P (Jaspart 1991) - see Fig. A1.4. This problem was first discussed by Timoshenko and Gere (1963). The critical value of P is given by

$$P_{\text{cr}} = \frac{4\pi D}{d_{\text{wc}}} \tag{A1.19}$$

and the flexural rigidity of the web plate D is

$$D = \frac{Et^3_{\text{wc}}}{12(1-\nu^2)} \tag{A1.20}$$

being ν: Poisson's coefficient.

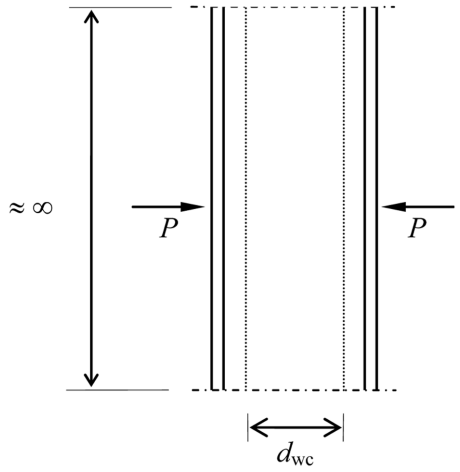

Fig. A1.4 Long rectangular plate of width d_{wc} subjected to opposite transverse forces

From Eq. (A1.16)

$$\bar{\lambda} = \sqrt{\frac{f_y}{\sigma_c}} = \sqrt{\frac{f_y A_p}{\sigma_c A_p}} = \sqrt{\frac{F_{pl}}{P_{cr}}} \tag{A1.21}$$

where A_p: plate cross-sectional area; and F_{pl}: plastic resistance of the plate, given by

$$F_{pl} = b_{eff,c,wc} t_{wc} f_{y,wc} \tag{A1.22}$$

For $\nu = 0.3$ (steel plate), then

$$\bar{\lambda} = \underbrace{\sqrt{\frac{12(1-0.3^2)}{4\pi}}}_{=0.932} \sqrt{\frac{b_{eff,c,wc} d_{wc} f_{y,wc}}{E t_{wc}^2}} = 0.932 \sqrt{\frac{b_{eff,c,wc} d_{wc} f_{y,wc}}{E t_{wc}^2}} \tag{A1.23}$$

which is equivalent to Eq. (A1.13).

A1.3 Stiffness formulae

According to EN 1993-1-8, the elastic stiffness coefficient of the column web in compression k_2 is obtained as

$$k_2 = \frac{0.7 b_{eff,c,wc} t_{wc}}{d_{wc}} \tag{A1.24}$$

whereby $b_{eff,c,wc}$ is the effective width from section A1.1.2. The background to this formula is given in Jaspart (1991) and Weynand *et al.* (1995).

The elastic stiffness is defined as the ratio between the compressive force F_{el} and the corresponding shortening $\Delta_{c,wc}$. Jaspart (1991) proposes the following relationship

$$F_{el} = b_{eff,el} t_{wc} E \frac{\Delta_{c,wc}}{d_{wc}} = b_{eff,el} t_{wc} E \varepsilon_{el} = b_{eff,el} t_{wc} E \frac{f_{y,wc}}{E} = b_{eff,el} t_{wc} f_{y,wc} \tag{A1.25}$$

in which $b_{eff,el}$ is the effective breadth in the elastic range. Weynand *et al.* (1995) adopt $b_{eff,el} = 2/3 b_{eff,c,wc}$. This value corresponds to the relation between the maximum elastic resistance and the pure plastic resistance of the component F_{pl}, computed in Eq. (A1.22).

Taking $F_{el} / F_{pl} = 2/3$, from Eqs. (A1.22) and (A1.24) the following relationship is obtained

$$b_{eff,el} = \frac{2}{3} b_{eff,c,wc} \approx 0.7 b_{eff,c,wc} \tag{A1.26}$$

Then

$$k_2 = \frac{F_{el}}{E \Delta_{c,wc}} = \frac{0.7 b_{eff,c,wc} t_{wc}}{d_{wc}} \tag{A1.27}$$

References

Aribert, J.M. and Lachal, A. (1977), "Étude élasto-plastique par analyse des contraintes de la compression locale sur l'âme d'un profilé", *Constr. Métallique*, **4**, 51-66.

Aribert, J.M., Lachal, A. and El Nawawy, O. (1981), "Modélisation élasto-plastique de la résistance d'un profilé en compression locale", *Constr. Métallique*, **2**, 3-26.

Aribert, J.M., Lachal, A. and Moheissen, M. (1990), "Interaction du voilement et de la résistance plastique de l'âme d'un profilé laminé soumis à une double compression locale (nuance dácier allant jusqu'à FeE460)", *Constr. Métallique*., **2**, 3-23.

Bathe, K.J. (1982), *Finite element procedures in engineering analysis*, Prentice-Hall, Englewood Cliffs, New Jersey.

Bathe, K.J. and Wilson, E.L. (1976), *Numerical methods in finite element analysis*, Prentice-Hall, Englewood Cliffs, New Jersey.

Bayo, E., Cabrero, J.M. and Gil, B. (2006), "An effective component-based method to model semi-rigid connections for the global analysis of steel and composite structures", *Eng. Struct.*, **28**, 97-108.

CEN - European committee for standardization (2005a), EN 1993-1-1 - *Eurocode* 3: *Design of steel structures – Part* 1-1: *General rules and rules for buildings*.

CEN - European Committee for Standardization (2005b), EN 1993-1-8 - *Eurocode* 3: *Design of steel structures - Part* 1-8: *Design of joints*.

CEN - European Committee for Standardization (2005c), EN 1993-1-12 - *Eurocode* 3: *Design of steel structures - Part* 1-12: *Additional rules for the extension of EN* 1993 *up to steel grades S*700.

CEN - European Committee for Standardization (2008), EN 1090-2 - *Execution of steel structures and aluminium structures - Part* 2*: Technical requirements for steel structures (corrected)*.

Chi, W.M., Kanvinde, A.M. and Deierlein, G.G. (2006), "Prediction of ductile fracture in steel connections using SMCS criterion", *J. Struct. Eng-ASCE*, **132**(2), 171-181.

De Mita, L., Piluso, V. and Rizzano, G. (2008), "Theoretical and experimental analysis of column web in compression", *Open. Constr. Build. Technol. J.*, **2**, 313-322.

Faella, C., Piluso, V. and Rizzano, G. (2000), *Structural semi-rigid connections - theory, design and software*, CRC Press, USA.

FEA (2006), LUSAS: *Finite element analysis system*, *Version* 14, Produced by FEA Ltd., Kinston-upon-Thames, Surrey.

Galambos, T.V. (1998), *Guide to stability design criteria for metal structures*, 5th edition, John Wiley and Sons, New York.

Gioncu, V. and Mazzolani, F.M. (2002), *Ductility of seismic resistant steel structures*, Spon Press, London, UK.

Girão Coelho, A.M. and Bijlaard, F.S.K. (2007a), "Experimental behaviour of high strength steel end plate connections", *J. Constr. Steel Res.*, **63**, 1228-1240.

Girão Coelho, A.M. and Bijlaard, F.S.K. (2007b), "Ductility of high strength steel moment connections", *Int. J. Adv. Steel Const.*, **3**(4), 765-783.

Girão Coelho, A.M. and Bijlaard, F.S.K., (2010), "Behaviour of high strength steel moment joints", *Heron*, **55**(1), 1-32.

Girão Coelho, A.M., Bijlaard, F.S.K. and Kolstein, H. (2009), "Experimental behaviour of high-strength steel web shear panels", *Eng. Struct.*, **31**, 1543-1555.

Jaspart, J.P. (1991), *Étude de la semi-rigidité des noeuds pouter-colonne et son influence sur la resistance et la stabilité des ossatures en acier*, Ph. D thesis (in French), University of Liège.

Jaspart, J.P. (1997), *Contributions to recent advances in the field of steel joints - column bases and further configurations for beam-to-column joints and beam splices*, Aggregation thesis, University of Liège.

Kuhlmann, U. (1999), *Influence of axial forces on the component* "*column web under compression*", Document Cost C1/WD2/99-01.

Kuhlmann, U. and Kühnemund, F. (2000a), "Rotation capacity of steel joints: verification procedure and component tests" *Proceedings of the NATO Advanced Research Workshop: The paramount role of joints into the reliable response of structures* (Eds.: CC Baniotopoulos and F Wald), Nato Science series, Kluwer Academic Publishers, Dordrecht, 363-372.

Kuhlmann, U. and Kühnemund, F. (2000b), "Procedures to verify rotation capacity", *Semi-rigid joints in structural steelwork* (Eds. Ivanyi, M., Baniotopoulos, C.C.), International Centre for Mechanical Sciences, 167-225.
Kuhlmann, U. and Kühnemund, F. (2002), "Ductility of semi-rigid steel joints" *Proceedings of the International Colloquium on Stability and Ductility of Steel Structures* (SDSS 2002) (Ed. Ivanyi, M.), Budapest, 363-370.
Kuhlmann, U., Davison, J.B. and Kattner, M. (1998), "Structural systems and rotation capacity", *Proceedings of the International Conference on Control of the Semi-Rigid Behaviour of Civil Engineering Structural Connections* (Ed. Maquoi, R.), Liège, 167-176.
Kühnemund, F. (2003), *On the verification of the rotation capacity of semi-rigid joints in steel structures*, Ph.D Thesis (in German), University of Stuttgart.
Owen, D.R.J. and Hinton, E. (1980), *Finite elements in plasticity, theory and practice*, Pineridge Press Limited, Swansea.
Skejic, D., Dujmovic, D. and Androic, B. (2008), "Reliability of the bending resistance of welded beam-to-column joints", *J. Constr. Steel Res.*, **64**, 388-399.
Simões da Silva, L. (2008), "Towards a consistent design approach for steel joints under generalized loadings", *J. Constr. Steel Res.*, **64**, 1059-1075.
Timoshenko, S.P. and Gere, J.M. (1963), *Theory of elastic stability*, 2nd edition, McGraw Hill, Singapore.
Weynand, K., Jaspart, J.P. and Steenhuis, M. (1995), "The stiffness model of revised Annex J of Eurocode 3", *Proceedings of the Third International Workshop on Connections in Steel Structures III, Behaviour, Strength and Design* (Eds. Bjorhovde, R., Colson, A., Zandonini, R.), Trento, 441-452.
Witteveen, J., Stark, J.W.B., Bijlaard, F.S.K. and Zoetemeijer, P. (1982), "Welded and bolted beam-to-column connections", *J. Struct. Div. ASCE*, **108**(2), 433-455.
Zoetemeijer, P. (1980), *The influence of normal-, bending- and shear stresses on the ultimate compression force exerted laterally to European rolled sections*, Stevin Laboratory Report 6-80-5, Faculty of Civil Engineering, Delft University of Technology.

DN